Supporting online information for

Generation of Ru(III)-hypochlorite with resemblance to heme dependent haloperoxidase enzyme‡

Rakesh Kumar,[a] Faiza Ahsan,[b] Ayushi Awasthi,[a] Marcel Swart[b,c*] and Apparao Draksharapu[a,*]

[a] Southern Laboratories - 208A, Department of Chemistry, Indian Institute of Technology Kanpur, Kanpur-208016 (India). appud@iitk.ac.in
[b] IQCC & Departament de Química, Universitat de Girona, 17003 Girona, Spain.
[c] ICREA, 08010, Barcelona, Spain. marcel.swart@gmail.com

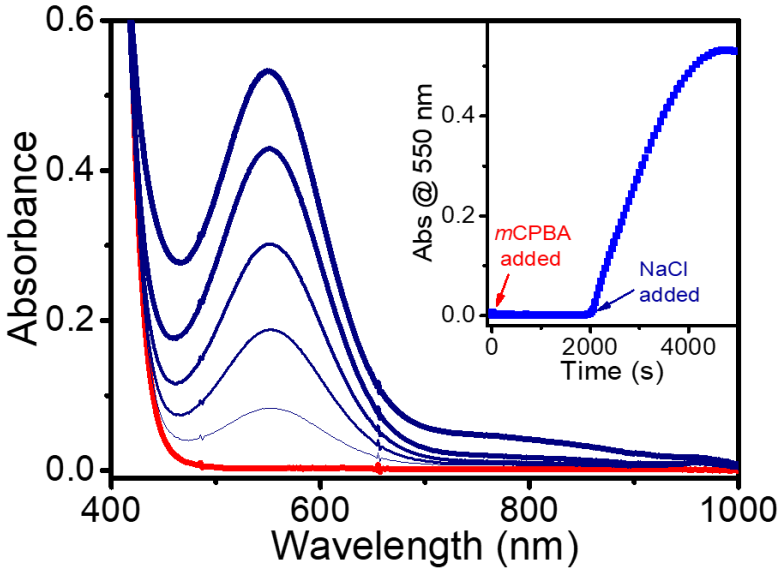

Fig. S1: (A) UV/Vis absorption spectral changes upon the reaction of 0.5 mM **1** (red) in 3:1 CH_3CN:H_2O with 20 eq. *m*CPBA (no spectral changes occurred) followed by 140 eq. aqueous NaCl (at ca. 2000 s) at room temperature. Inset: The corresponding absorption changes at 550 nm.

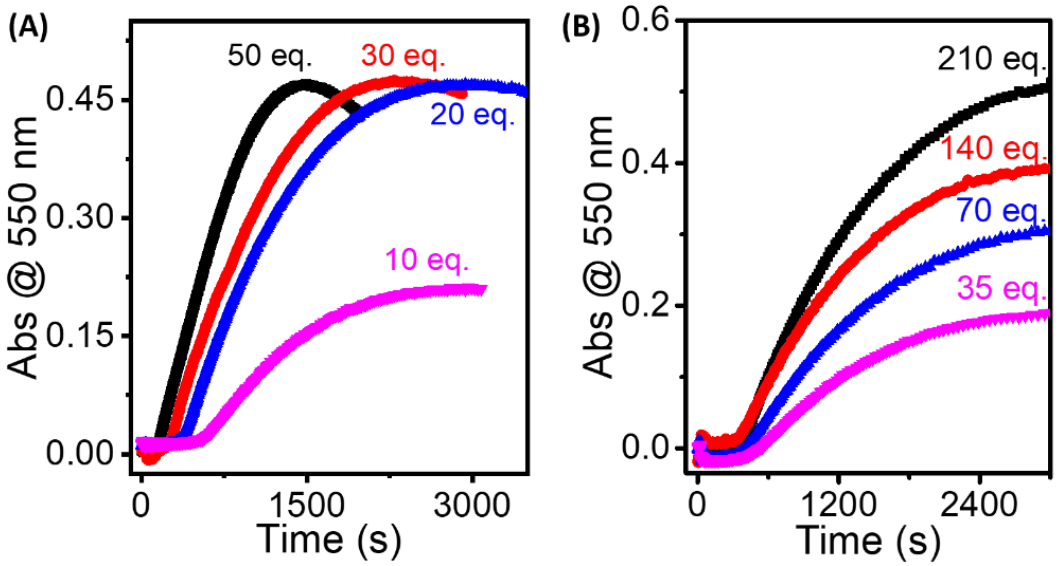

Fig. S2: (A) Time-dependent absorption changes at 550 nm upon the reaction of 0.5 mM **1** in 3:1 CH_3CN:H_2O (A) with different eq. (10, 20, 30, and 50) of *m*CPBA and 140 eq. aqueous NaCl, and (B) with different eq. (35, 70, 140, 210, 280) of aqueous NaCl and 20 eq. *m*CPBA at room temperature.

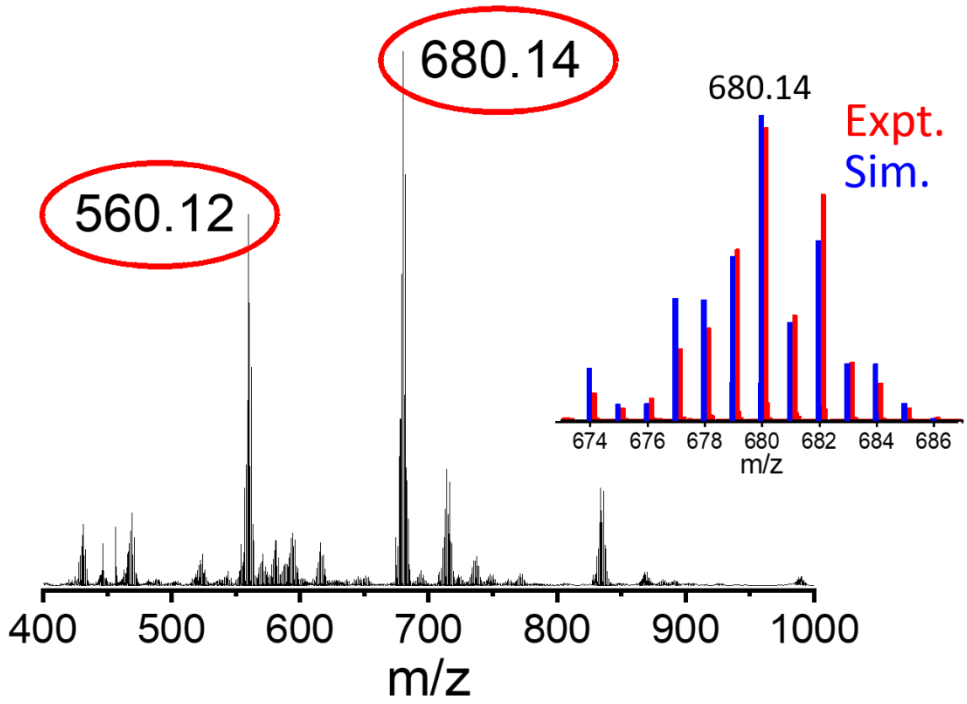

Fig. S3: Positive mode ESI-mass data of **2**, generated upon the reaction of **1** with 20 eq. of *m*CPBA and 140 eq. of aqueous NaCl in 3:1 CH_3CN:H_2O at room temperature.

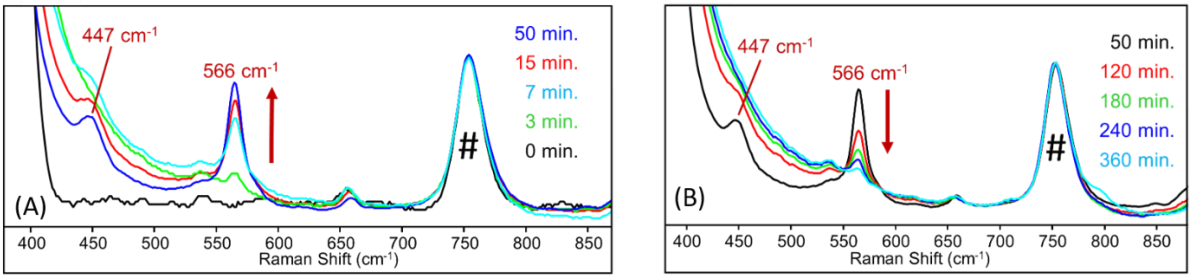

Fig. S4: Time-dependent resonance Raman spectra (at λ_{exc} 561 nm) for the (A) formation and (B) decay of **2** in 3:1 CH_3CN:H_2O generated by adding 20 eq. of *m*CPBA and 140 eq. of aqueous NaCl to **1** at room temperature. # Indicates solvent peak.

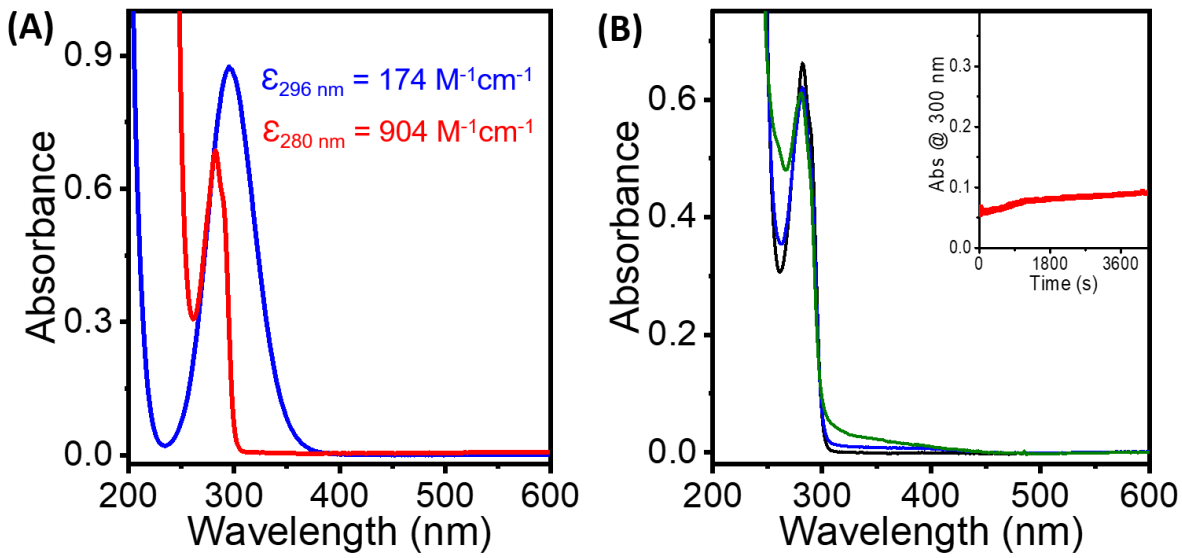

Fig. S5: (A) UV/Vis absorption spectra of 5 mM NaOCl (blue) and 0.75 mM *m*CPBA (red). (B) The reaction of *m*CPBA with 70 eq. aqueous NaCl in MeCN: H_2O (3:1) at room temperature followed by UV/Vis absorption spectroscopy. Inset: The corresponding absorption changes at 300 nm.

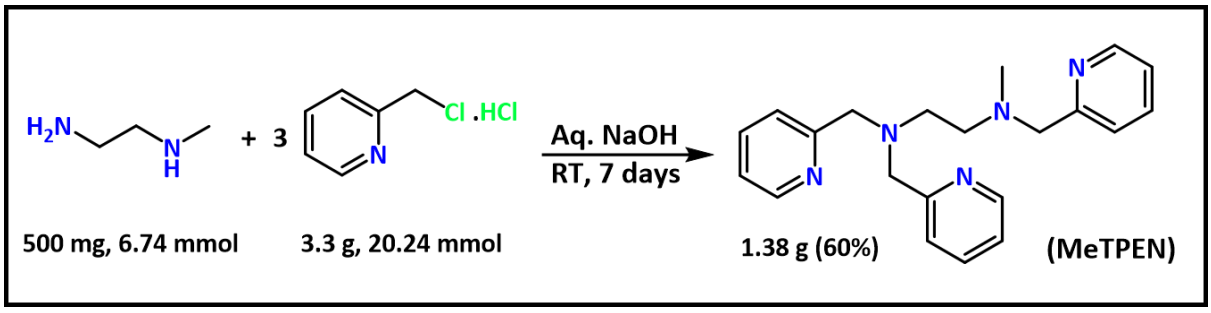

Scheme S1: Synthetic procedure for MeTPEN ligand.

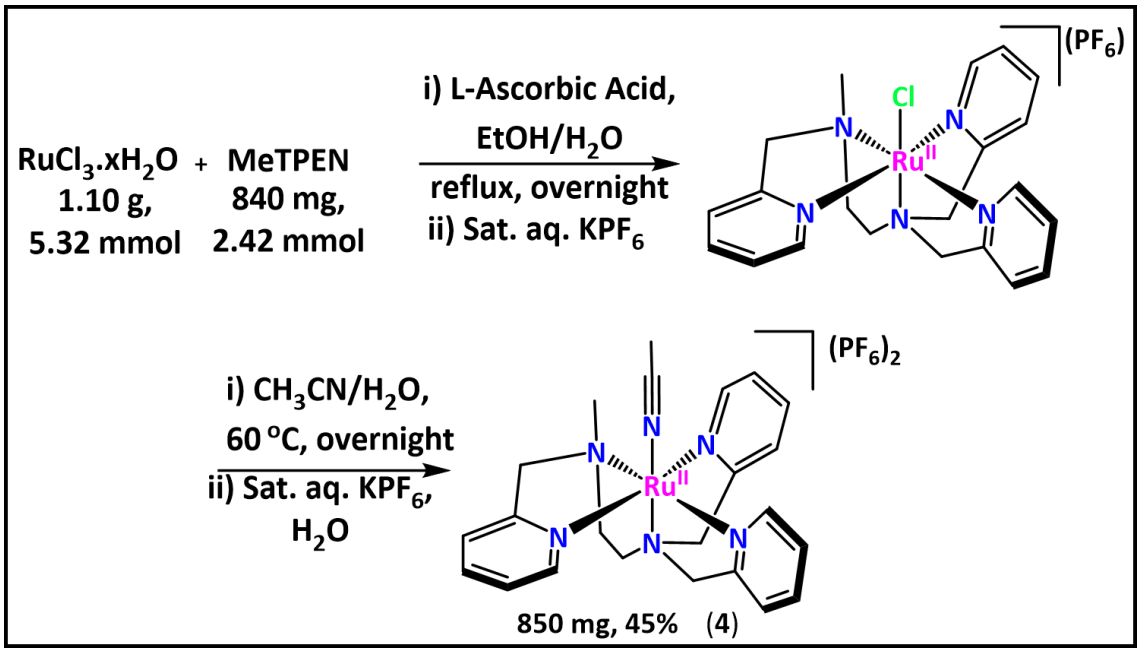

Scheme S2: Synthetic procedure for $[Ru^{II}(MeTPEN)(NCCH_3)](PF_6)_2$ (**4**).

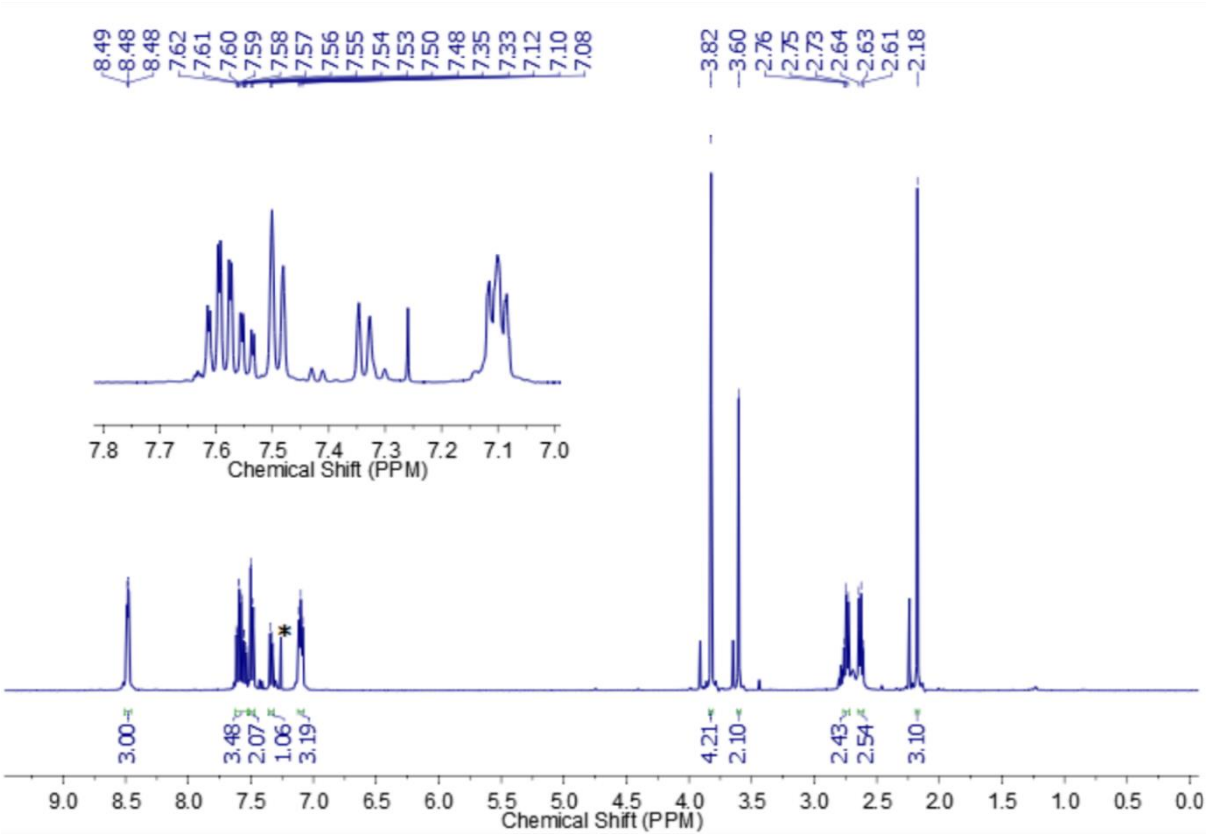

Fig. S6: ^{1}H NMR spectrum of MeTPEN in $CDCl_3$ at 400 MHz. (* peak for solvent)

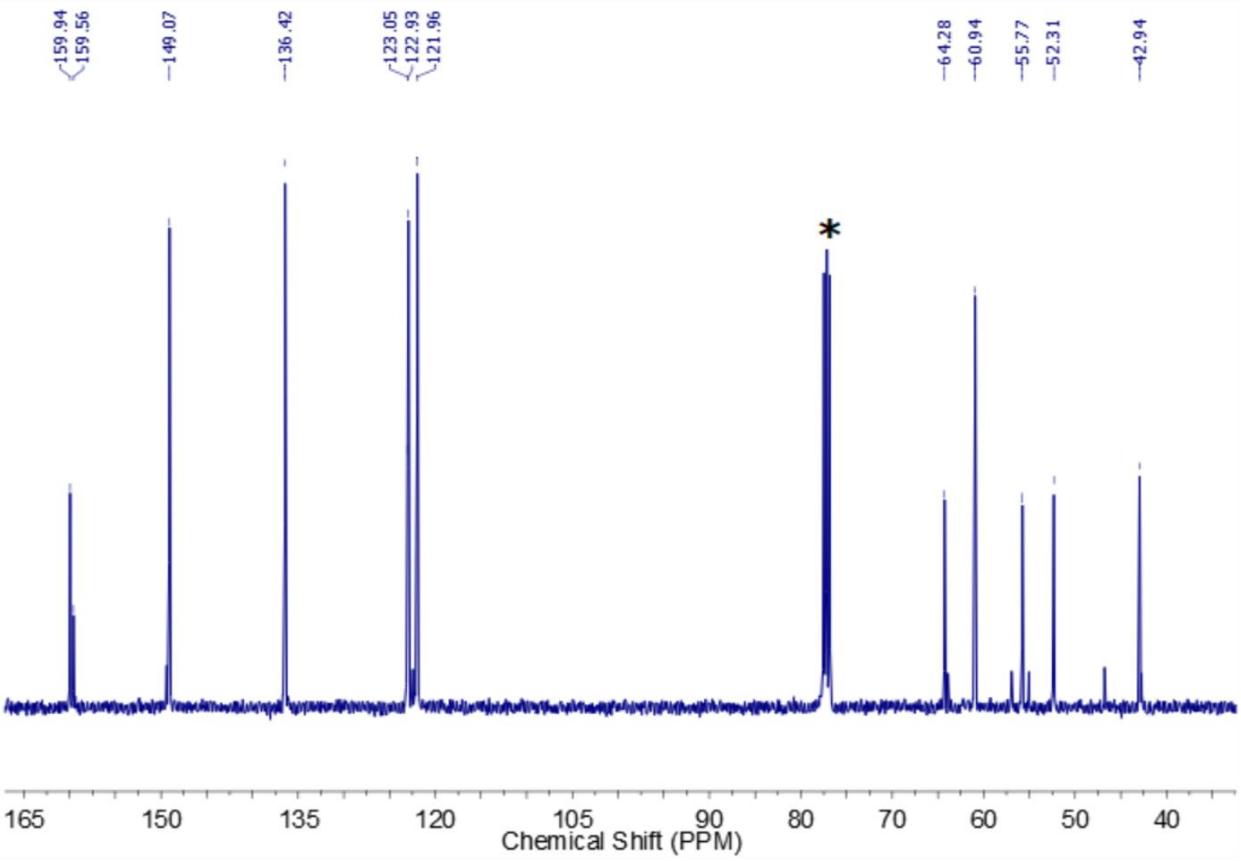

Fig. S7: ^{13}C NMR spectrum of MeTPEN in $CDCl_3$ at 100 MHz. (* peak for solvent)

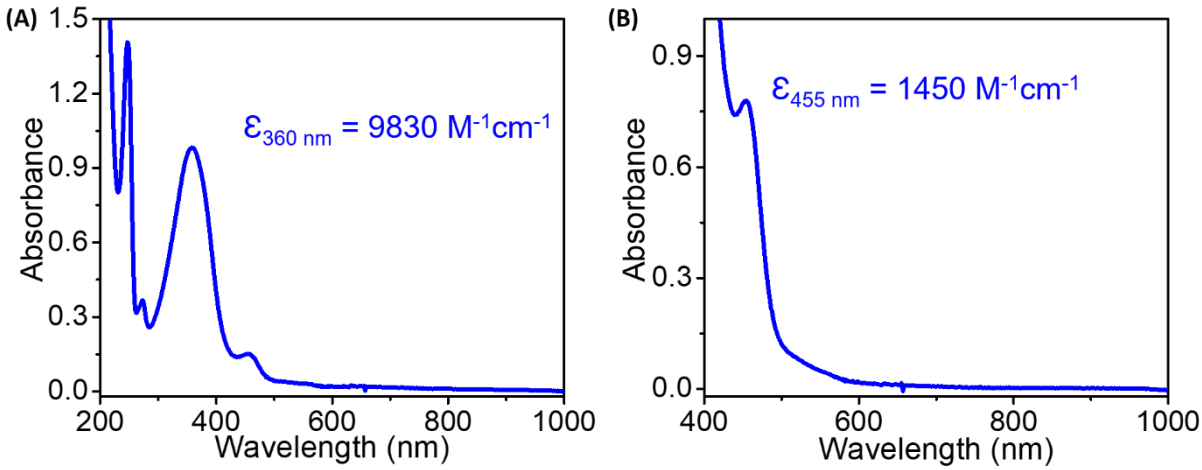

Fig. S8: UV/Vis absorption spectra (A) 0.1 mM and (B) 0.5 mM of **4** in CH_3CN at room temperature.

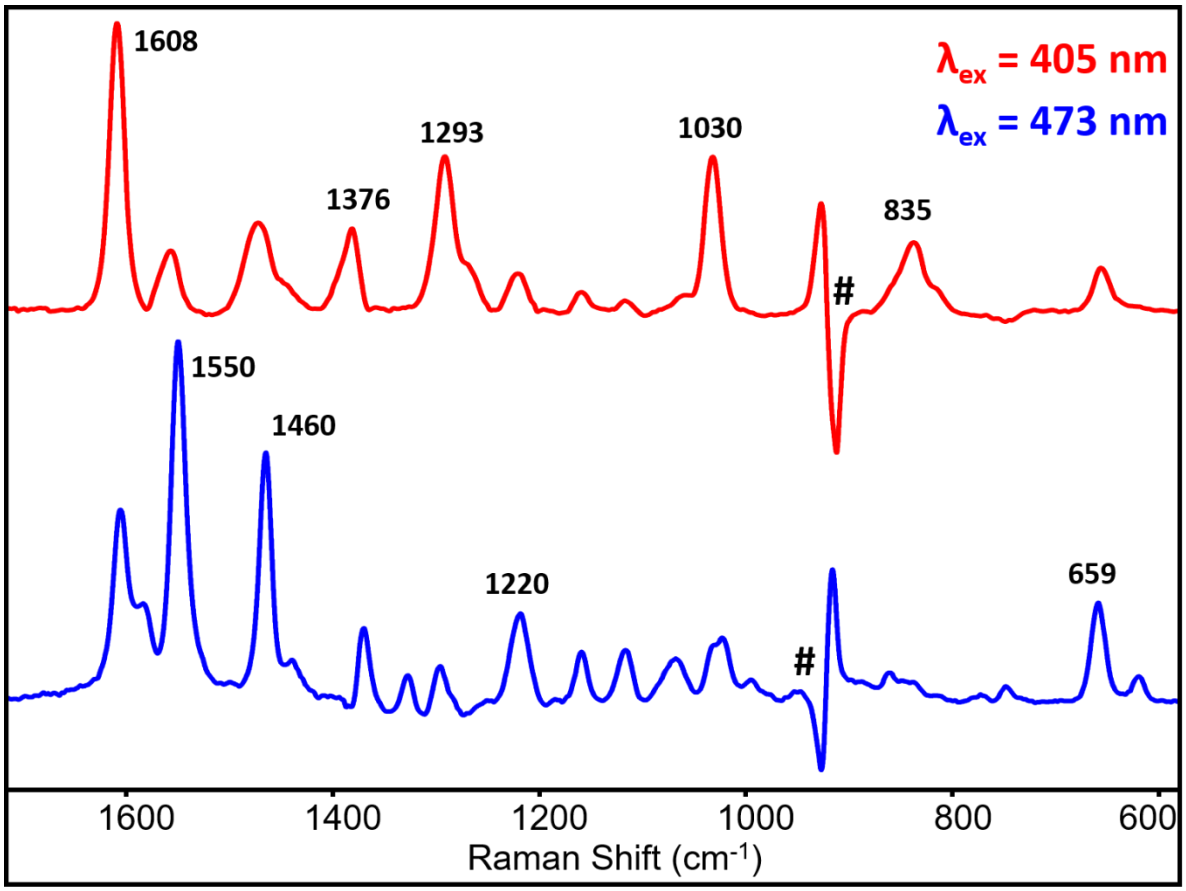

Fig. S9: Solvent subtracted resonance Raman spectrum of 0.5 mM **4** in acetonitrile at λ_{exc} = 405 nm (red) and 473 nm (blue). [#]Indicate imperfect solvent subtraction.

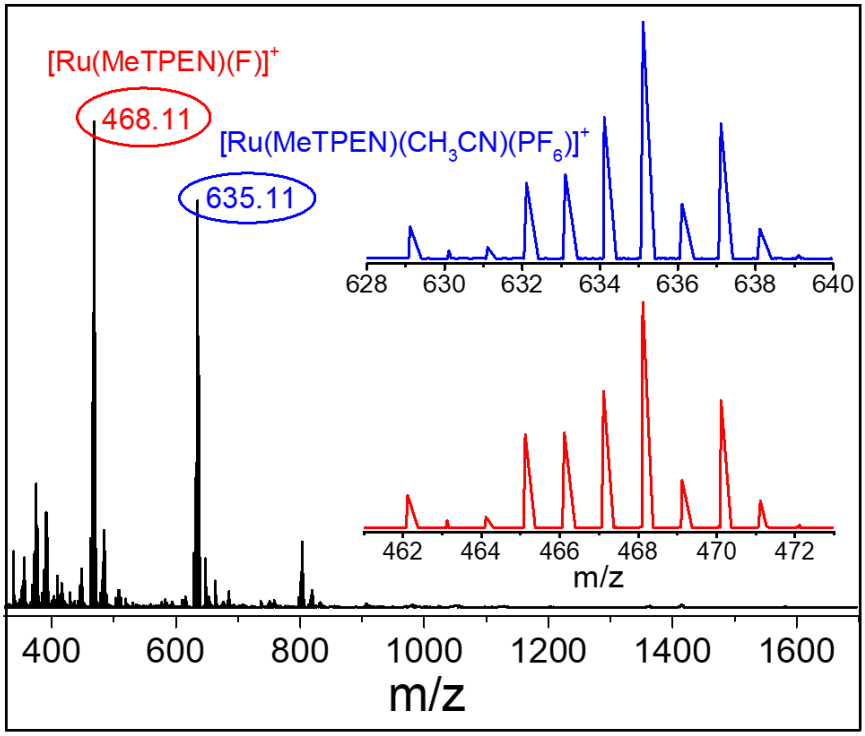

Fig. S10: Positive mode ESI-mass spectrum of **4** in CH_3CN.

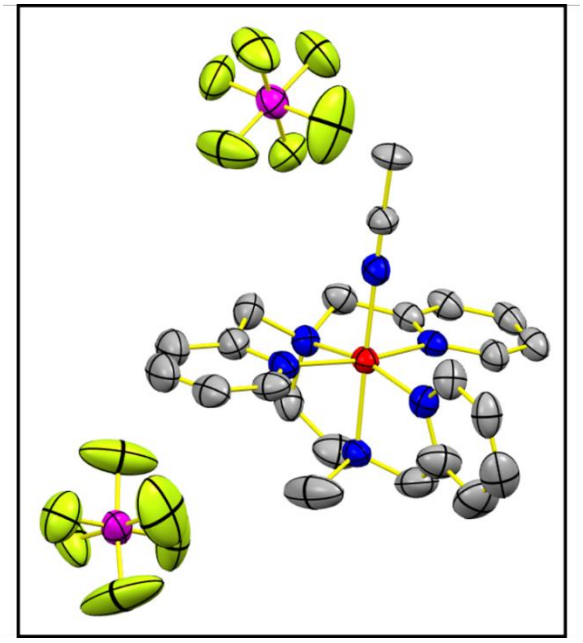

Fig. S11: X-ray crystal structure of $[Ru^{II}(MeTPEN)(NCCH_3)](PF_6)_2$ (**4**). Hydrogen atoms were omitted for clarity.

Table S1: Crystal data and structure refinement of **4**.

Empirical formula	$C_{23}H_{28}F_{12}N_6P_2Ru$
Formula weight	779.52
Temperature/K	100
Crystal system	monoclinic
Space group	$P2_1/c$
a/Å	13.1578(15)
b/Å	11.6873(13)
c/Å	19.140(2)
α/°	90
β/°	103.637(4)
γ/°	90
Volume/Å^3	2860.3(6)
Z	4
ρ_{calc}g/cm^3	1.810
μ/mm^{-1}	0.766
F(000)	1560.0
Crystal size/mm^3	0.19 × 0.17 × 0.16
Radiation	MoKα (λ = 0.71073)
2Θ range for data collection/°	4.878 to 56.698
Index ranges	-17 ≤ h ≤ 17, -15 ≤ k ≤ 15, -25 ≤ l ≤ 25
Reflections collected	43525
Independent reflections	7131 [R_{int} = 0.1260, R_{sigma} = 0.0852]
Data/restraints/parameters	7131/0/399
Goodness-of-fit on F^2	0.984
Final R indexes [I>=2σ (I)]	R_1 = 0.0755, wR_2 = 0.1900
Final R indexes [all data]	R_1 = 0.1349, wR_2 = 0.2407
Largest diff. peak/hole / e Å^{-3}	1.26/-1.12

Table S2: Selected Bond lengths (Å) of **1**, **4** and bond distance comparison with $[Ru^{II}(TPA)(NCCH_3)_2](PF_6)_2$ and $[Ru^{II}(N4Py)(OH_2)](PF_6)_2$.[1, 2]

	1	**4**	**$[Ru^{II}(TPA)(NCCH_3)_2](PF_6)_2$[a]**	**$[Ru^{II}(N4Py)(OH_2)](PF_6)_2$[b]**
Atom	**Length/Å**	**Length/Å**	**Length/Å**	**Length/Å**
$Ru\text{-}N_{py}$	2.067(3) 2.060(3) 2.071(3)	2.051(6) 2.066(6) 2.068(6)	2.062(4) 2.071(4) 2.056(4)	2.057(4) 2.052(4) 2.061(4) 2.060(5)
$Ru\text{-}N_{amine}$	2.069(3) 2.141(2)	2.087(6) 2.079(6)	2.053(4)	1.967(5)
$Ru\text{-}N_{MeCN}$	2.030(3)	2.041(6)	2.031(5) 2.037(5)	
$Ru\text{-}O_{water}$				2.172(5)
$Ru\text{-}N_{Avg}$	2.073	2.066	2.051	2.039

[a] TPA: tris(2-pyridylmethyl)amine;

[b] N4Py: N,N-bis(2-pyridyl-methyl)-N-bis(2-pyridyl)methylamine)

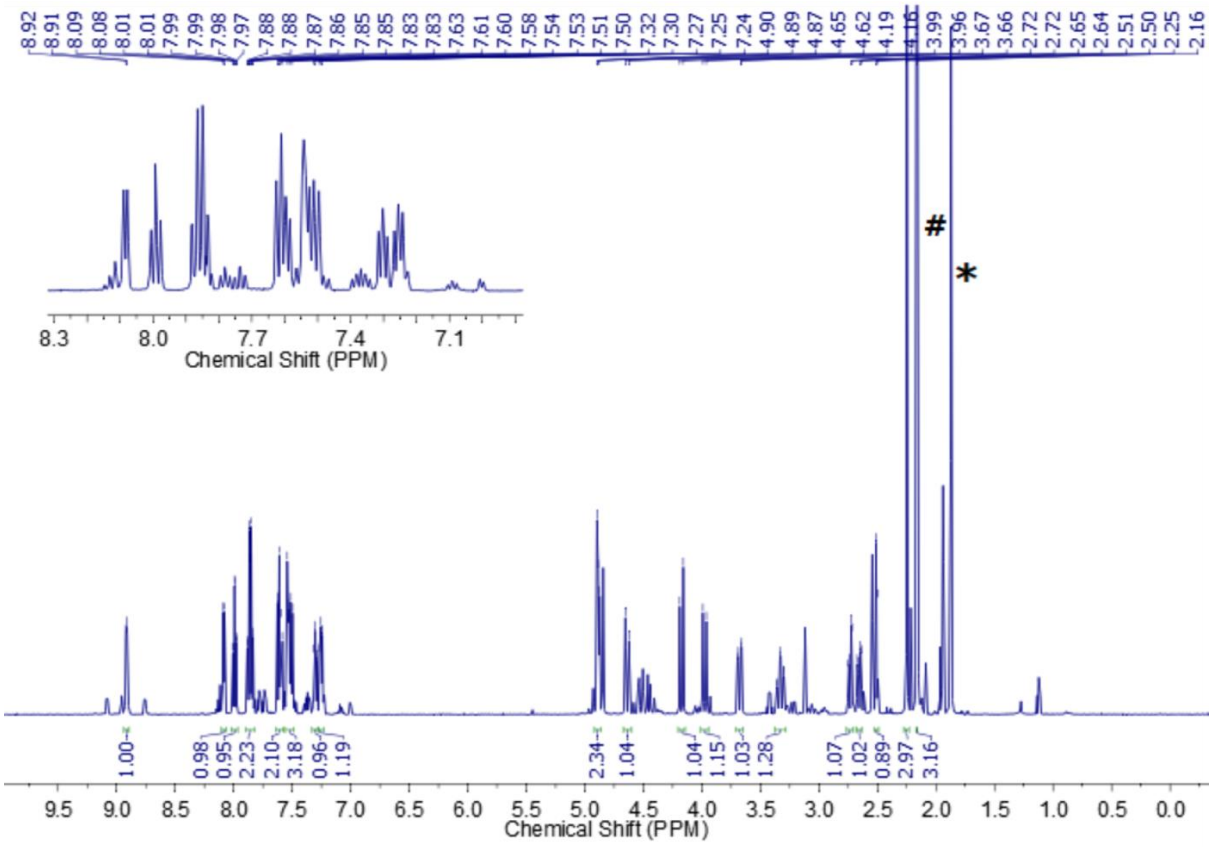

Fig. S12: ^1H NMR spectrum of **4** in CD_3CN at 500 MHz. (*peak for solvent, #peak for H_2O)

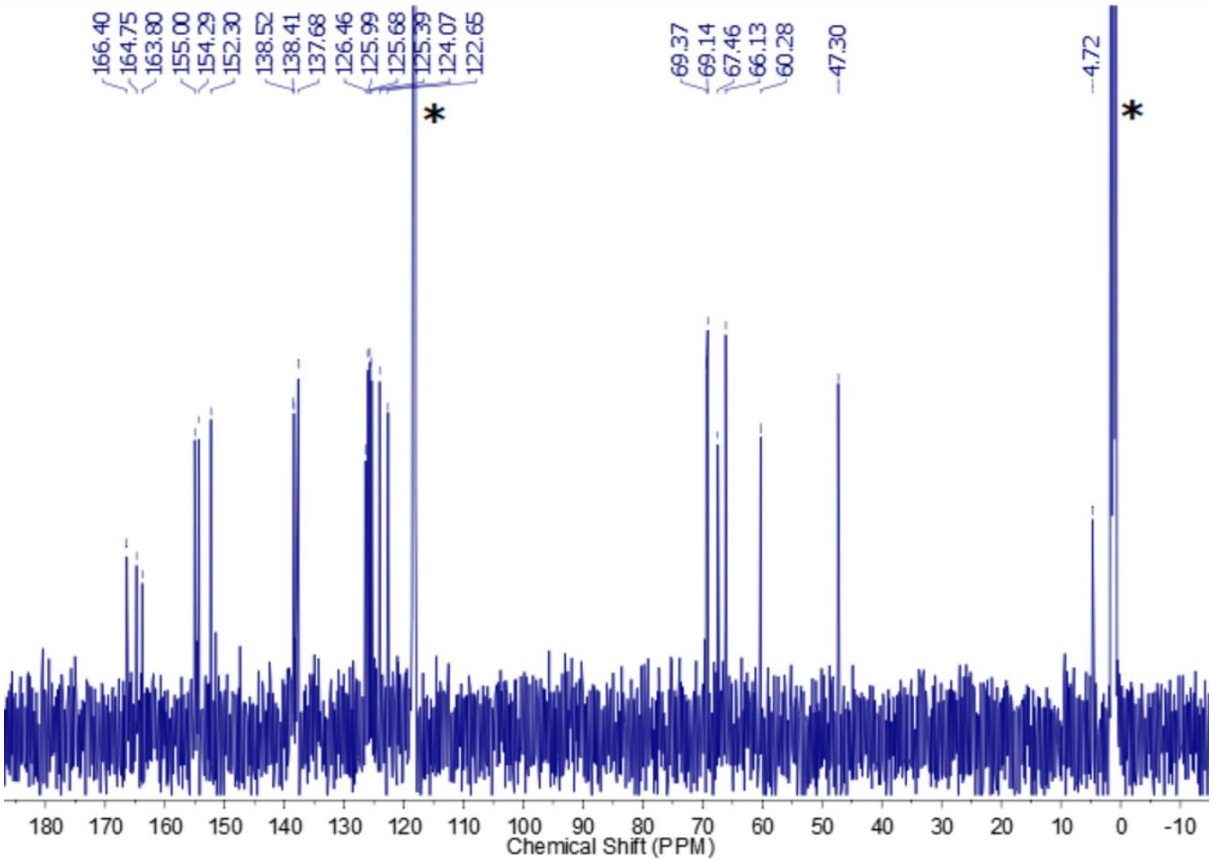

Fig. S13: ^{13}C NMR spectrum of **4** in CD_3CN at 125 MHz. (*peak for solvent)

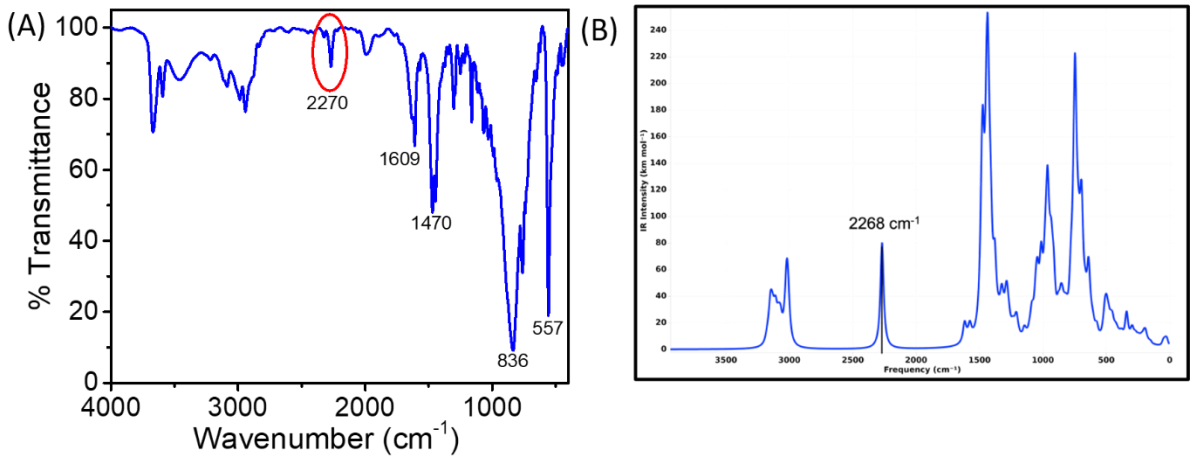

Fig. S14: (A) Solid-state FT-IR spectrum of **4** on KBr pellet. The band at 2270 cm^{-1} is originated from the bound acetonitrile ligand. (B) Computationally calculated IR spectrum of **4** and 2268 cm^{-1} band corresponds to the bound acetonitrile ligand.

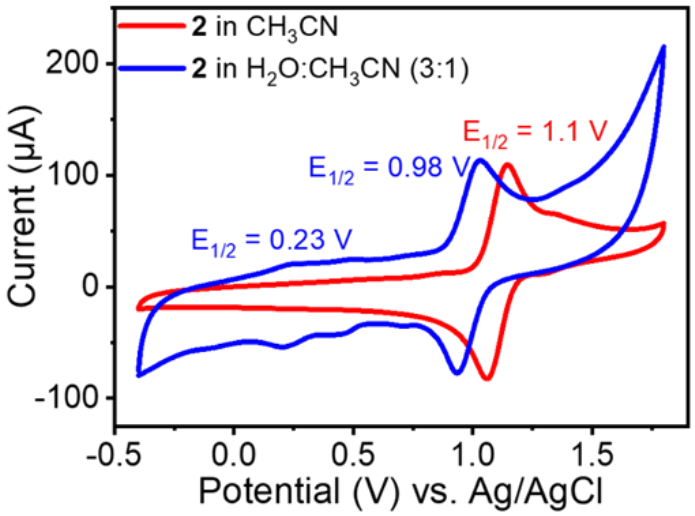

Fig. S15: Cyclic voltammograms of **4** in CH_3CN (red) and in 3 : 1 H_2O :CH_3CN (blue) at room temperature (scan rate 500 mV s^{-1}).

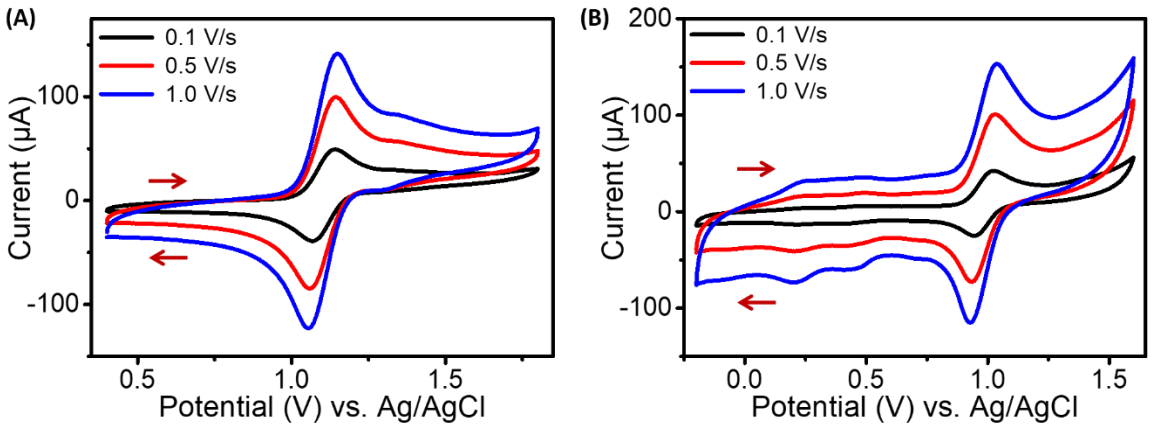

Fig. S16: Scan rate (in V/s) dependent cyclic voltammograms of **4** (A) in CH_3CN, and (B) in H_2O:CH_3CN (3:1).

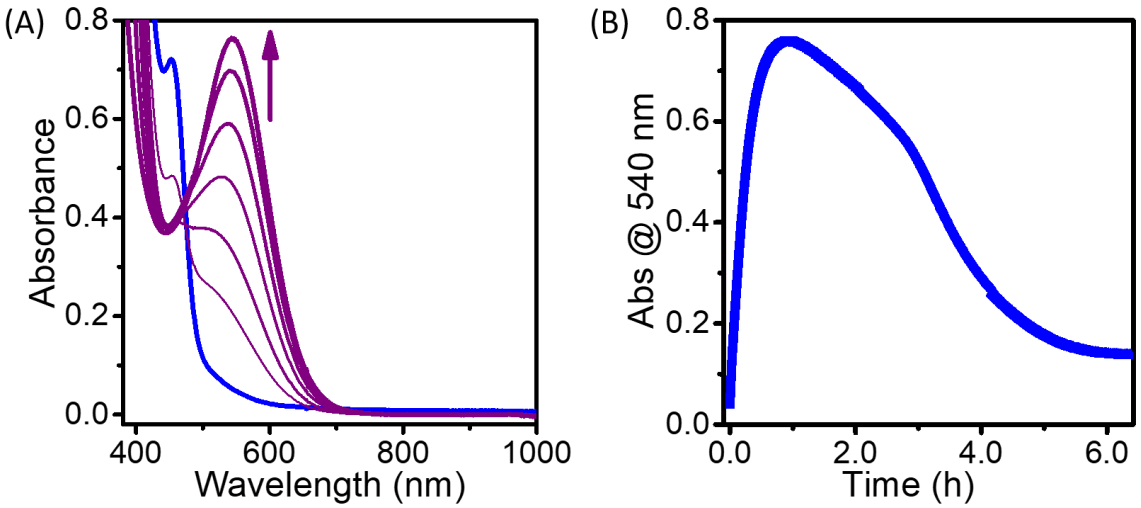

Fig. S17: (A) UV/Vis absorption spectral changes upon the reaction of 0.5 mM **4** in 3:1 $CH_3CN:H_2O$ with 10 eq. $HClO_4$ and 10 eq. aqueous NaOCl at room temperature give rise to 540 nm band. (B) The corresponding absorption changes at 540 nm. The intermediate persisted for 4.5 h under these conditions.

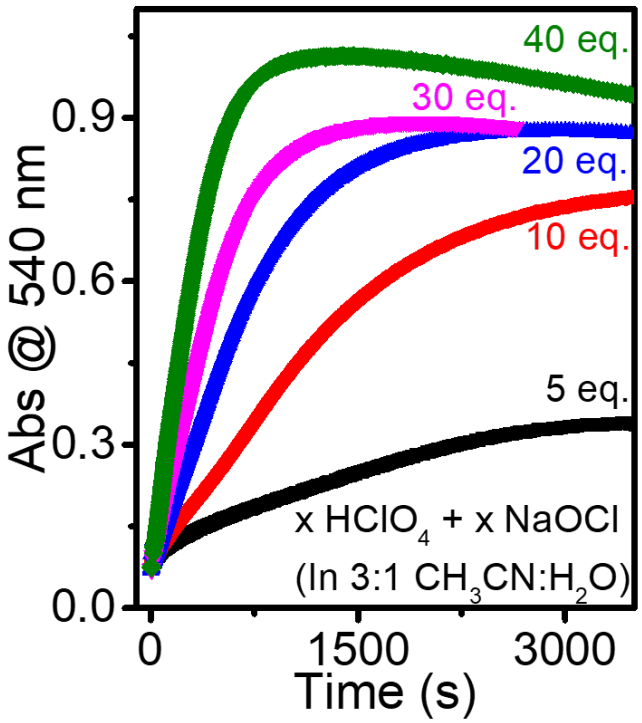

Fig. S18: Time-dependent absorption changes at 540 nm upon reaction of 0.5 mM **4** in 3:1 $CH_3CN:H_2O$ with different eq. (5, 10, 20, 30, and 40) of $HClO_4$ and aqueous NaOCl at room temperature.

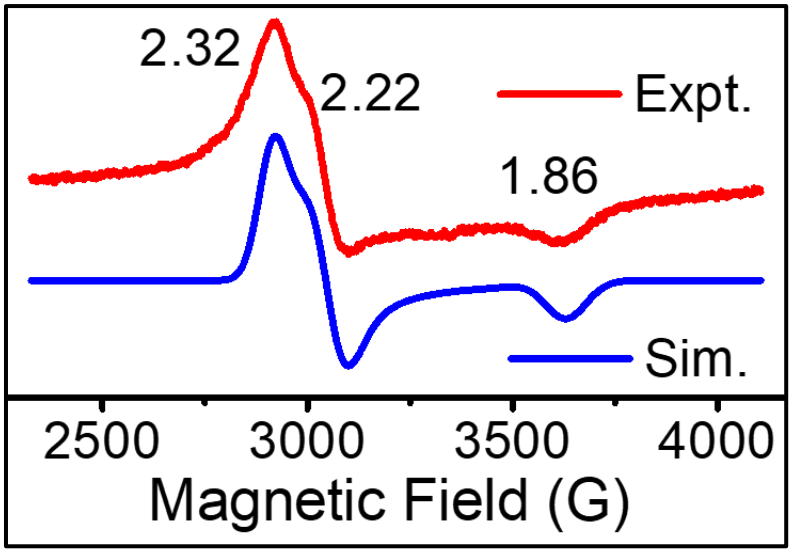

Fig. S19: Experimental (red) and simulated (blue) X-band EPR (9.45 GHz) spectrum of **5** (g_z = 2.32, g_y = 2.22 and g_x = 1.86) measured at 120 K; Modulation amplitude 5 G; Modulation frequency 100 KHz, and Attenuation 10 dB. *Condition to generation **5**: 0.5 mM **4** in 3:1 CH_3CN:H_2O with 10 eq. $HClO_4$ and 10 eq. aqueous NaOCl at room temperature.*

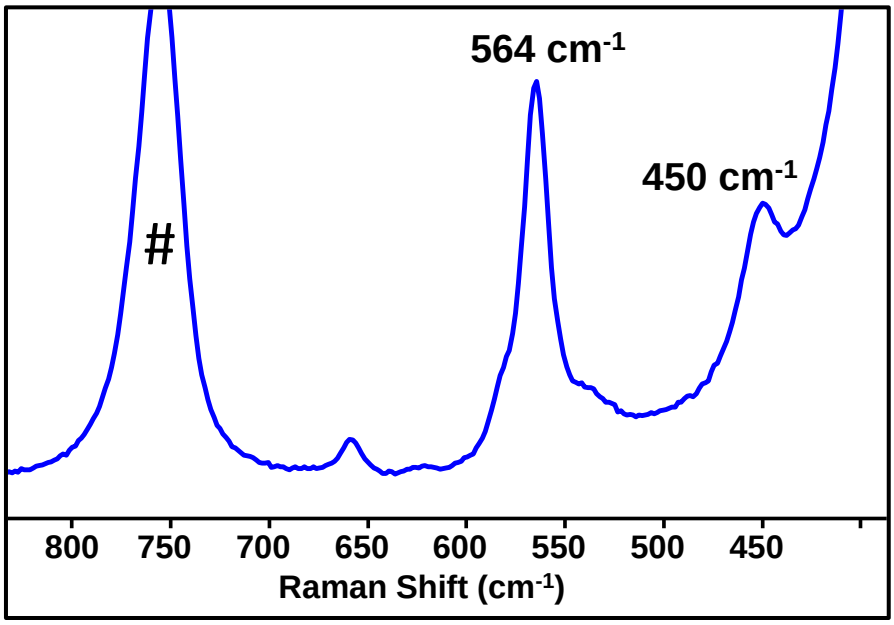

Fig. S20: Resonance Raman spectrum of **5** in MeCN: H_2O (3:1) obtained at λ_{exc} 561 nm. # Indicate solvent band. *Conditions to generate **5**: 0.5 mM **4** in 3:1 CH_3CN:H_2O with 10 eq. $HClO_4$ and 10 eq. aqueous NaOCl at room temperature.*

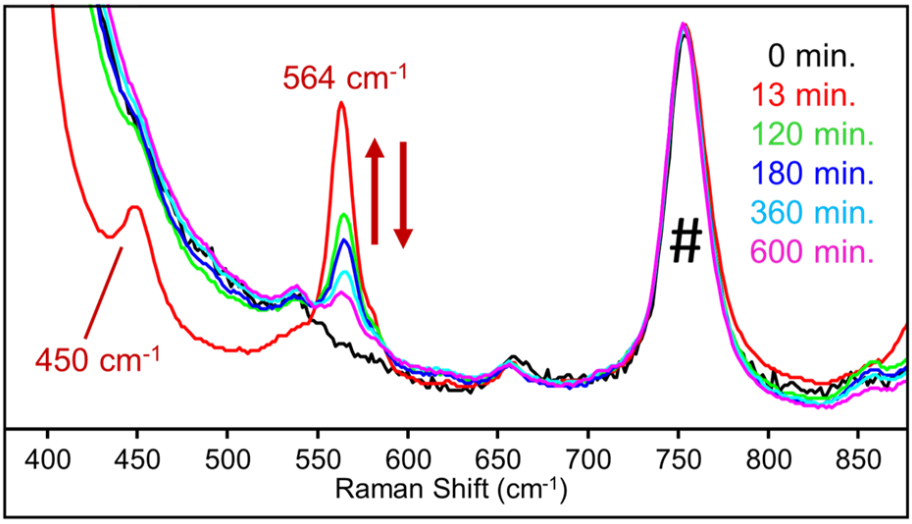

Fig. S21: Time-dependent resonance Raman spectra (at λ_{exc} 561 nm) of **5** in 3:1 $CH_3CN:H_2O$ generated by adding 20 eq. of *m*CPBA and 140 eq. of aqueous NaCl to **4** at room temperature. # Indicates solvent peak.

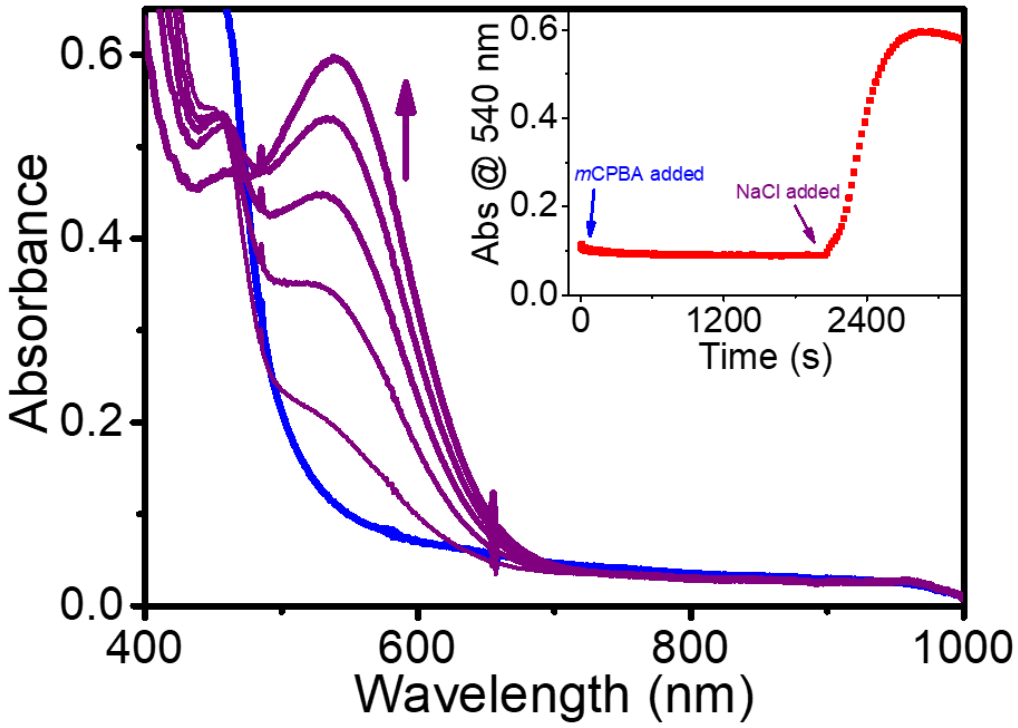

Fig. S22: UV/Vis absorption spectral changes upon the reaction of 0.5 mM **4** (Blue) in 3:1 $CH_3CN:H_2O$ with 20 eq. *m*CPBA and 140 eq. aqueous NaCl at room temperature give rise to 540 nm band. Inset: The corresponding absorption changes at 540 nm with time.

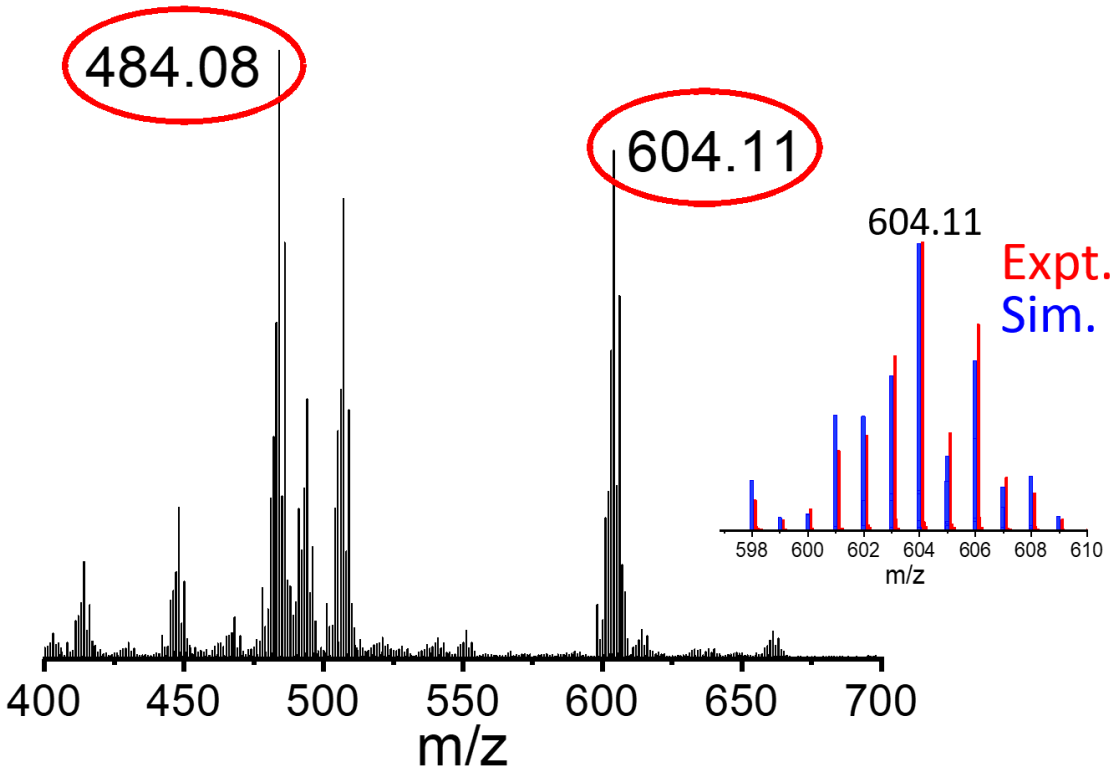

Fig. S23: Positive mode ESI-mass data of **5**, generated upon the reaction of **4** with 20 eq. of *m*CPBA and 140 eq. of aqueous NaCl in 3:1 CH_3CN:H_2O at room temperature.

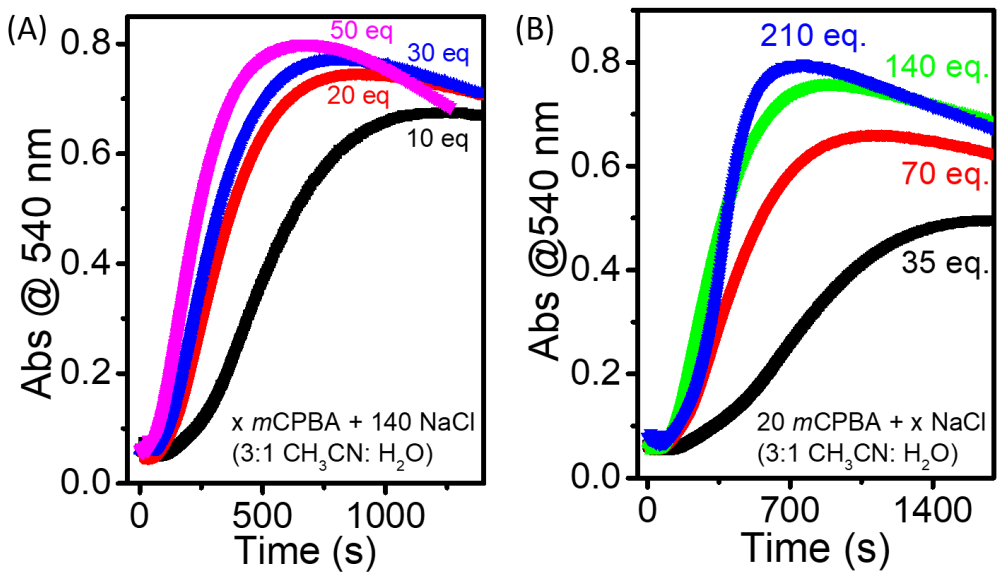

Fig. S24: Time-dependent absorption changes at 540 nm upon reaction of 0.5 mM **4** in 3:1 CH_3CN:H_2O, (A) with different eq. (10, 20, 30, 50) of *m*CPBA and 140 eq. aqueous NaCl, and (B) with different eq. (35, 70, 140, 210) of aqueous NaCl and 20 eq. *m*CPBA at room temperature.

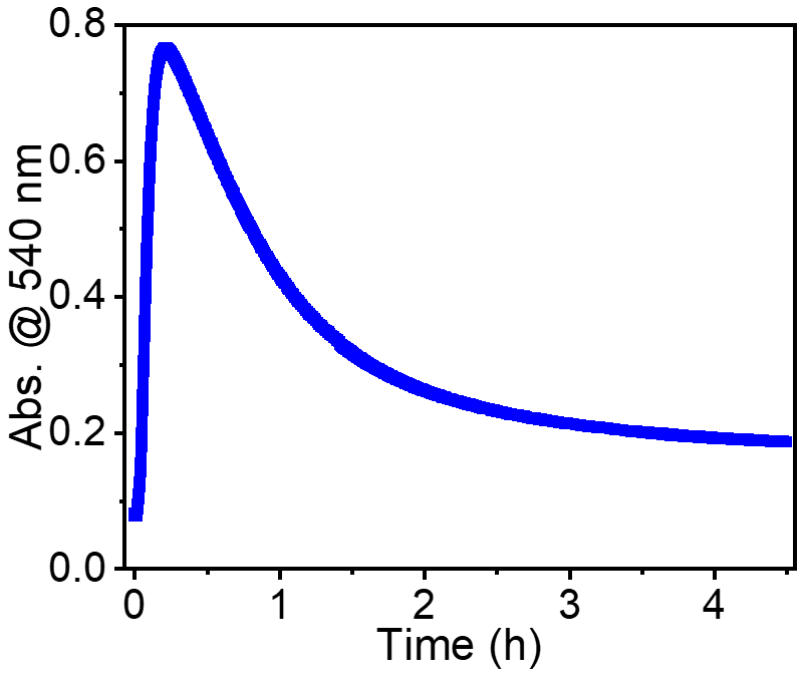

Fig. S25: Time-dependent absorption changes at 540 nm of **5**, generated upon the reaction of 0.5 mM **4** with 20 eq. *m*CPBA and 140 eq. aqueous NaCl in 3:1 CH_3CN:H_2O at room temperature. The intermediate persisted for 1.5 h under these conditions.

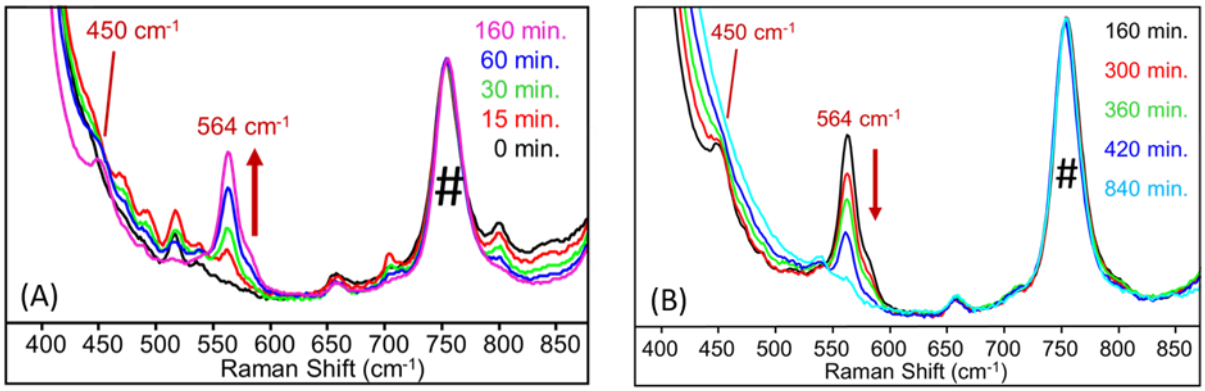

Fig. S26: Time-dependent resonance Raman spectra (at λ_{exc} 561 nm) for the (A) formation and (B) decay of **5** in 3:1 CH_3CN:H_2O generated by the addition of 10 eq. of NaOCl and 10 eq. of $HClO_4$ to **4** at room temperature. # Indicates solvent peak.

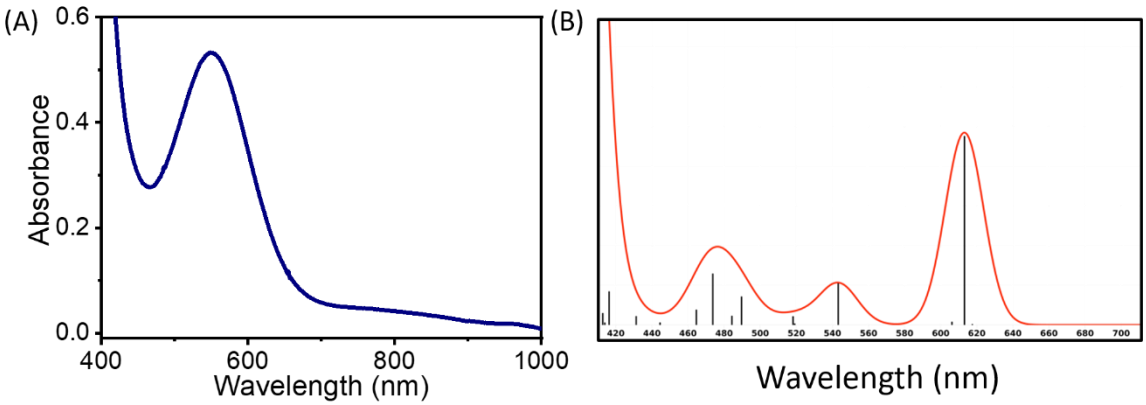

Fig. S27: (A) Experimentally obtained UV/Vis absorption spectrum of **2** in MeCN:H_2O (3:1). *Conditions to generate **2**: 0.5 mM **1** in MeCN:H_2O (3:1 v/v) + 20 eq. mCPBA + 140 eq. aqueous NaCl at RT.* (B) Computed absorption spectrum of **2**.

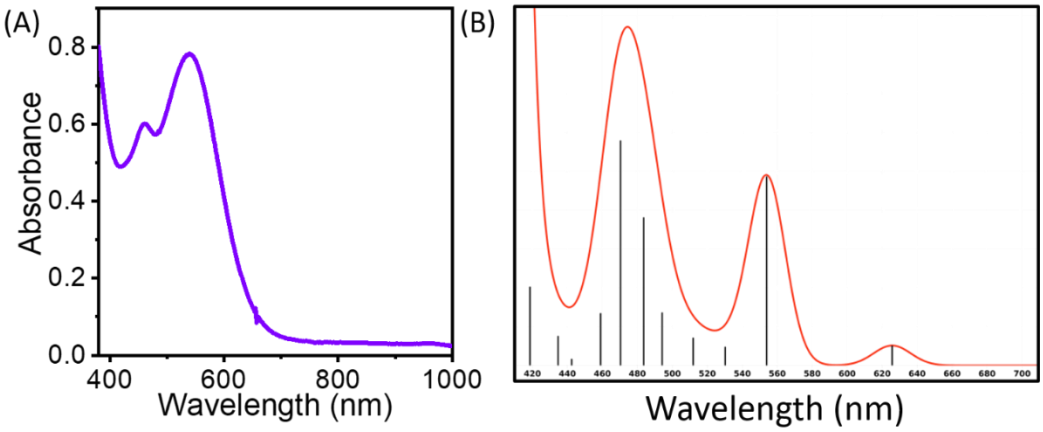

Fig. S28: (A) Experimentally obtained UV/Vis absorption spectrum of **5** in MeCN:H_2O (3:1). *Conditions to generate **5**: 0.5 mM **4** in MeCN:H_2O (3:1 v/v) + 20 eq. mCPBA + 140 eq. aqueous NaCl at RT.* (B) Computed absorption spectrum of **5**.

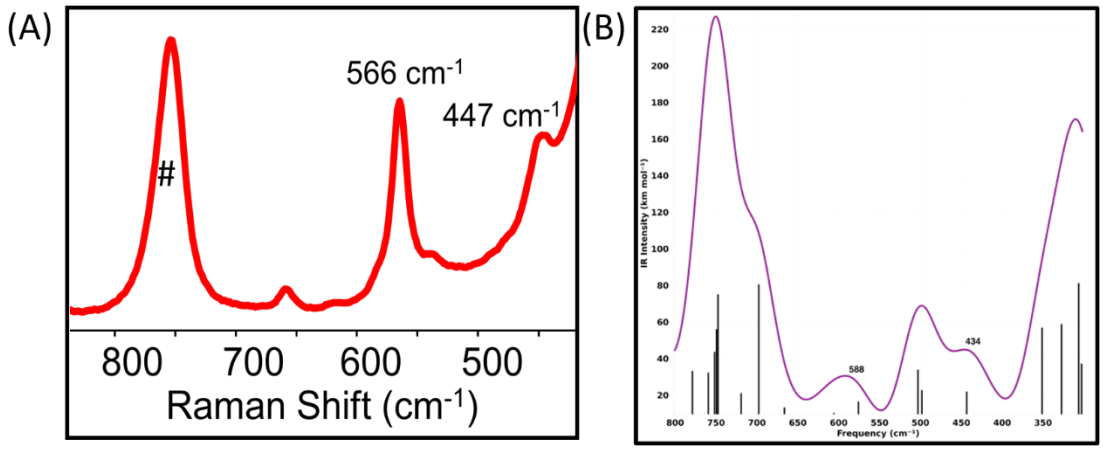

Fig. S29: (A) Experimentally obtained resonance Raman spectrum of **2** in MeCN:H_2O (3:1) obtained at λ_{exc} 561 nm. # Indicate solvent band. (B) Computed IR Spectrum of **2**.

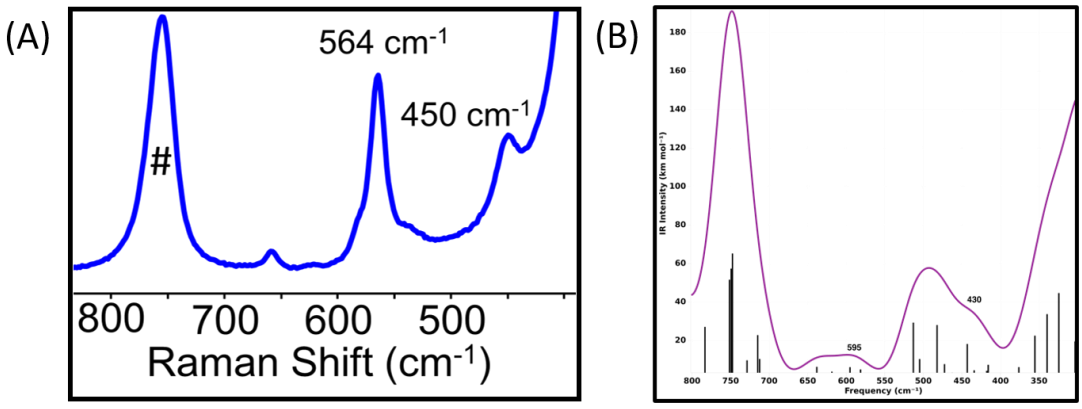

Fig. S30: (A) Experimentally obtained resonance Raman spectrum of **5** in MeCN:H_2O (3:1) obtained at λ_{exc} 561 nm. # Indicate solvent band. (B) Computed IR Spectrum of **5**.

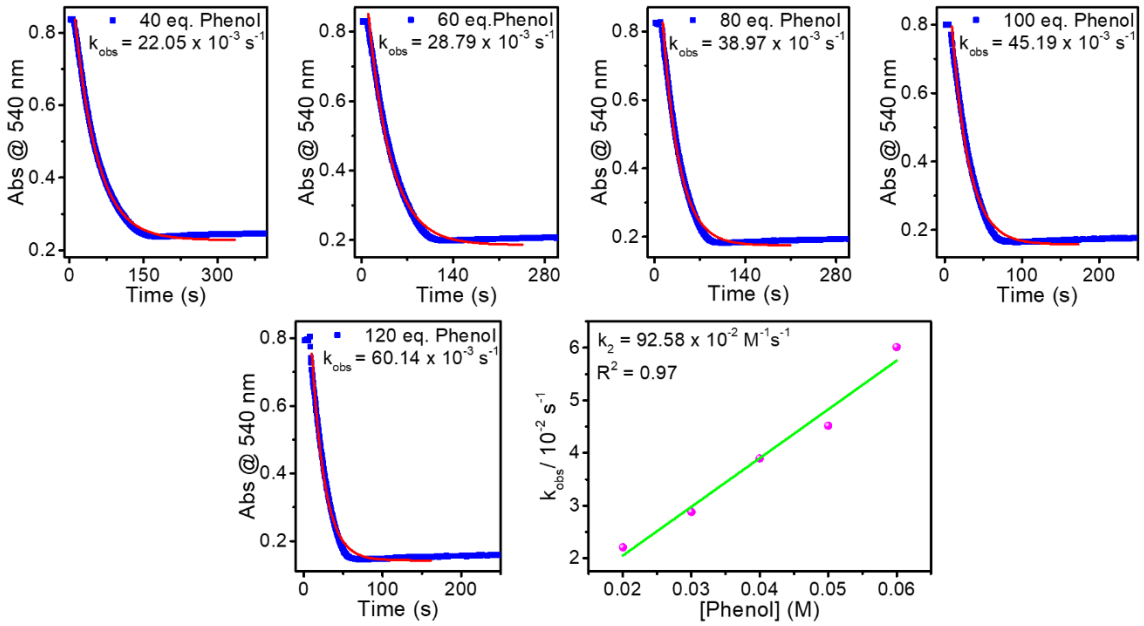

Fig. S31: Decay of **5** followed at 540 nm in presence of various concentrations of phenol to give pseudo-first-order rate constants (k_{obs}) in 3:1 CH_3CN: H_2O at 25 °C. The plot of k_{obs} against the concentrations of phenol to obtain a second-order-rate constant (k_2 = 92.58 x 10^{-2} $M^{-1}s^{-1}$). *Conditions to generate **5**: 0.5 mM **4** in 3:1 CH_3CN:H_2O + 20 eq. mCPBA and 140 eq. aqueous NaCl.*

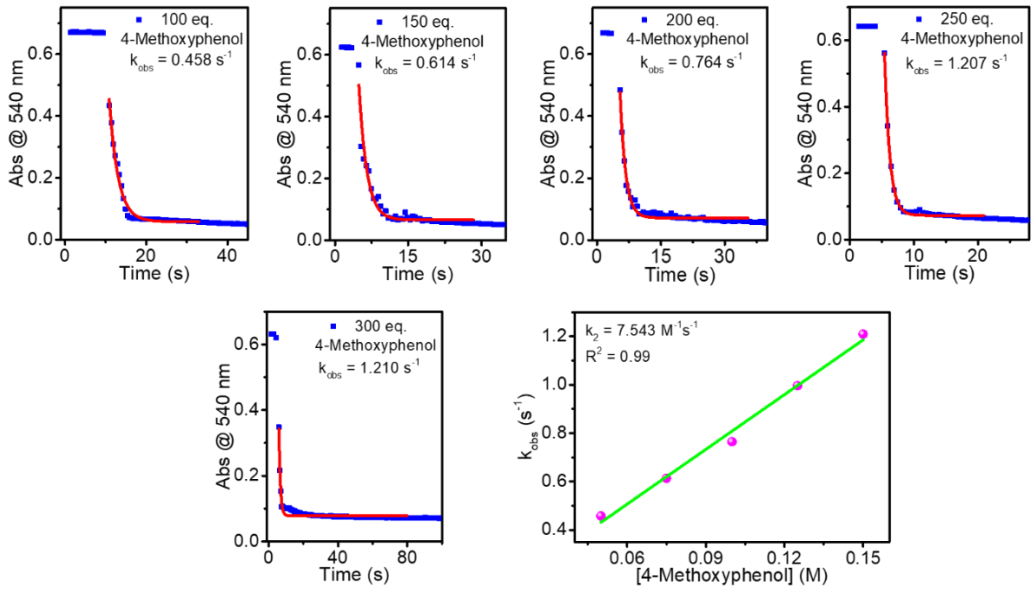

Fig. S32: Decay of **5** followed at 540 nm in presence of various concentrations of 4-methoxyphenol to give pseudo-first-order rate constants (k_{obs}) in 3:1 CH_3CN: H_2O at 25 °C. The plot of k_{obs} against the concentrations of 4-methoxyphenol to obtain a second-order-rate constant (k_2 = 7.543 $M^{-1}s^{-1}$). *Conditions to generate **5**: 0.5 mM **4** in 3:1 CH_3CN:H_2O + 20 eq. mCPBA and 140 eq. aqueous NaCl.*

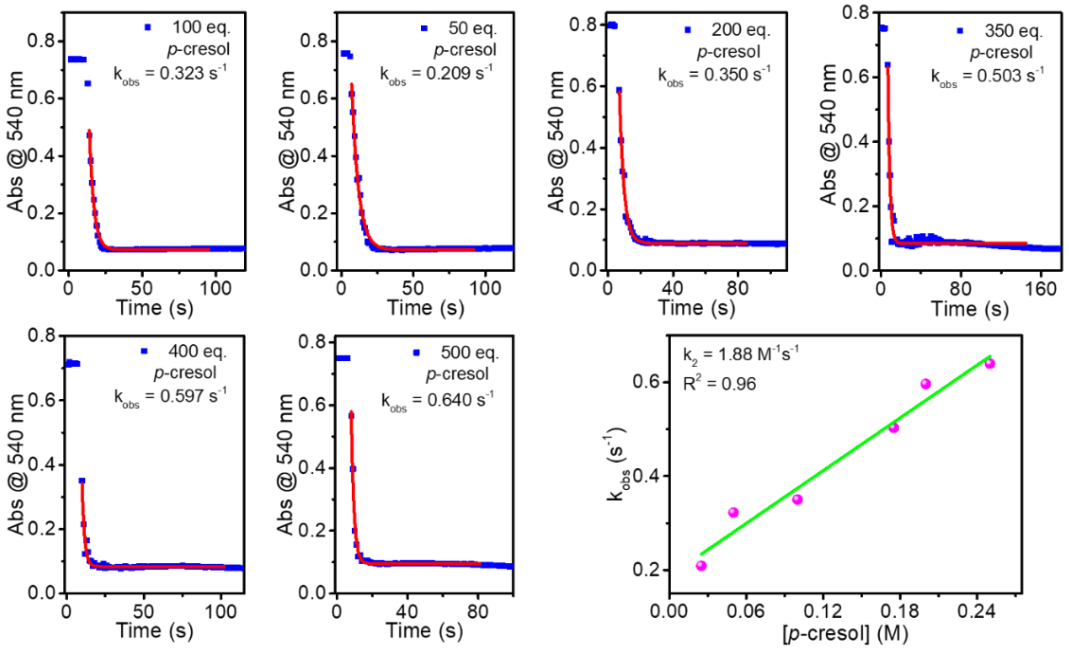

Fig. S33: Decay of **5** followed at 540 nm in presence of various concentrations of *p*-cresol to give pseudo-first-order rate constants (k_{obs}) in 3:1 CH_3CN: H_2O at 25 °C. The plot of k_{obs} against the concentrations of *p*-cresol to obtain a second-order-rate constant (k_2 = 1.88 $M^{-1}s^{-1}$). *Conditions to generate **5**: 0.5 mM **4** in 3:1 CH_3CN:H_2O + 20 eq. mCPBA and 140 eq. aqueous NaCl*.

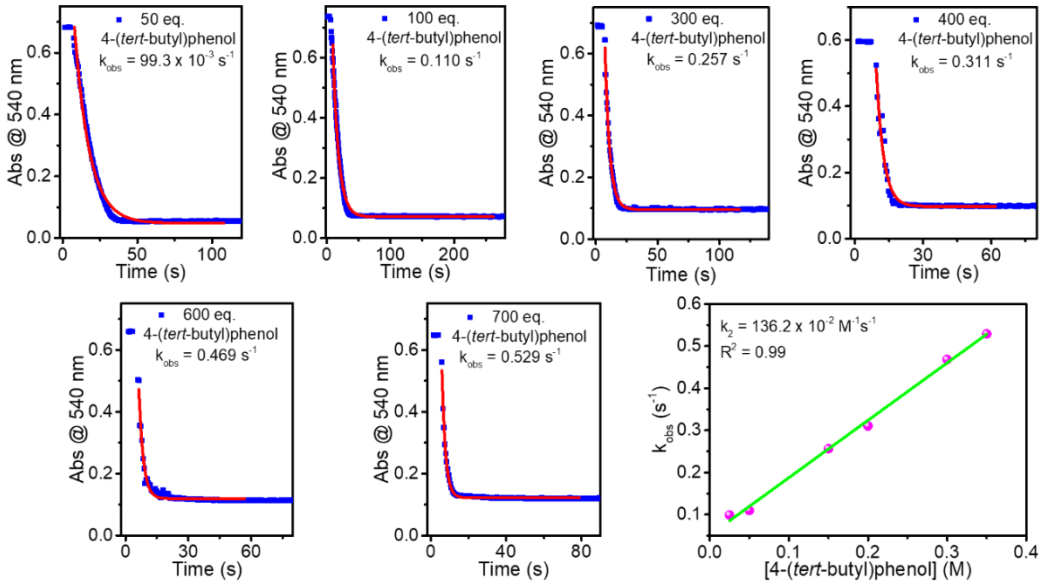

Fig. S34: Decay of **5** followed at 540 nm in presence of various concentrations of 4-(*tert*-butyl)phenol to give pseudo-first-order rate constants (k_{obs}) in 3:1 CH_3CN: H_2O at 25 °C. The plot of k_{obs} against the concentrations of 4-(*tert*-butyl)phenol to obtain a second-order-rate constant (k_2 = 1.362 $M^{-1}s^{-1}$). *Conditions to generate **5**: 0.5 mM **4** in 3:1 CH_3CN:H_2O + 20 eq. mCPBA and 140 eq. aqueous NaCl.*

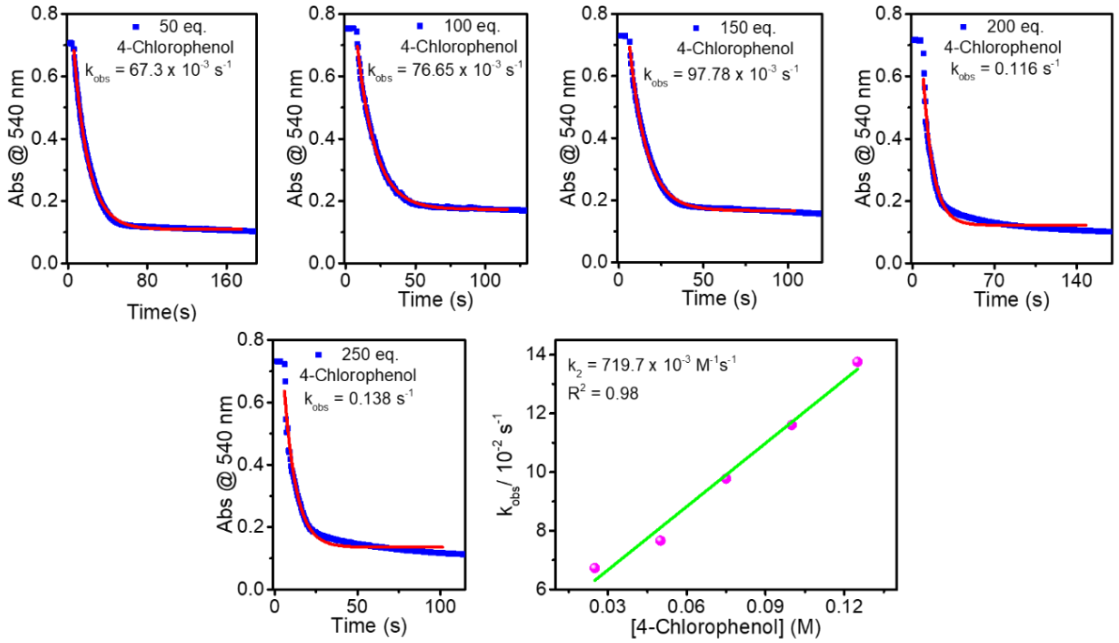

Fig. S35: Decay of **5** followed at 540 nm in presence of various concentrations of 4-chlorophenol to give pseudo-first-order rate constants (k_{obs}) in 3:1 CH_3CN: H_2O at 25 °C. The plot of k_{obs} against the concentrations of 4-chlorophenol to obtain a second-order-rate constant (k_2 = 719.7 x 10^{-3} $M^{-1}s^{-1}$). *Conditions to generate **5**: 0.5 mM **4** in 3:1 CH_3CN:H_2O + 20 eq. mCPBA and 140 eq. aqueous NaCl.*

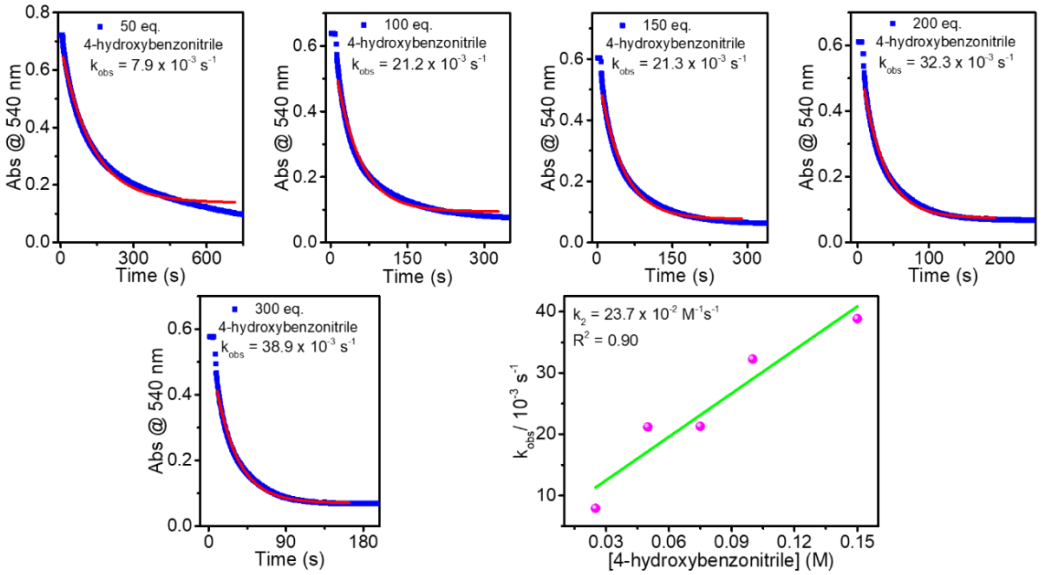

Fig. S36: Decay of **5** followed at 540 nm in presence of various concentrations of 4-hydroxybenzonitrile to give pseudo-first-order rate constants (k_{obs}) in 3:1 CH_3CN: H_2O at 25 °C. The plot of k_{obs} against the concentrations of 4-hydroxybenzonitrile to obtain a second-order-rate constant (k_2 = 23.7 x 10^{-2} $M^{-1}s^{-1}$). *Conditions to generate **5**: 0.5 mM **4** in 3:1 CH_3CN:H_2O + 20 eq. mCPBA and 140 eq. aqueous NaCl.*

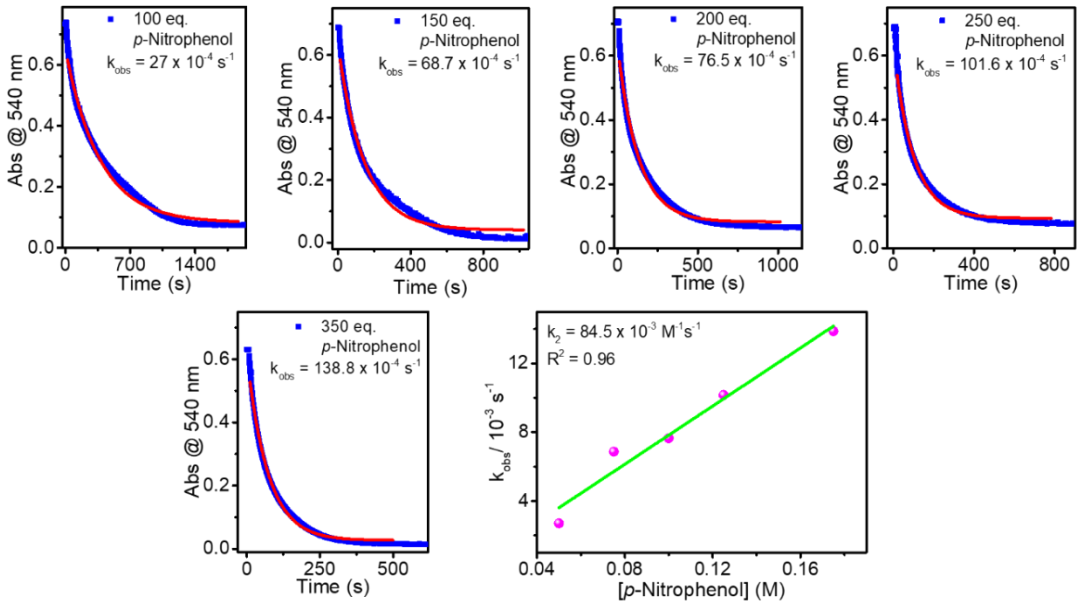

Fig. S37: Decay of **5** followed at 540 nm in presence of various concentrations of *p*-nitrophenol to give pseudo-first-order rate constants (k_{obs}) in 3:1 CH_3CN: H_2O at 25 °C. The plot of k_{obs} against the concentrations of *p*-nitrophenol to obtain a second-order-rate constant (k_2 = 84.5 x 10^{-3} $M^{-1}s^{-1}$). *Conditions to generate **5**: 0.5 mM **4** in 3:1 CH_3CN:H_2O + 20 eq. mCPBA and 140 eq. aqueous NaCl.*

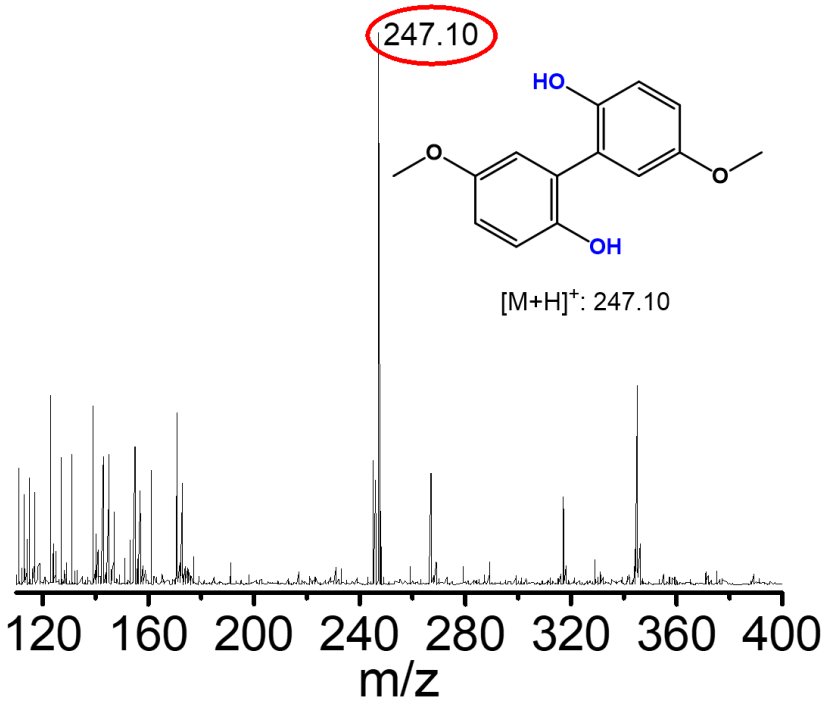

Fig. S38: Product analysis of the reaction of **5** with 50 eq. 4-methoxyphenol by APCI-MS. *Conditions to generate **5**: 2.0 mM **4** in 3:1 CH_3CN:H_2O + 20 eq. mCPBA and 140 eq. aqueous NaCl at room temperature.*

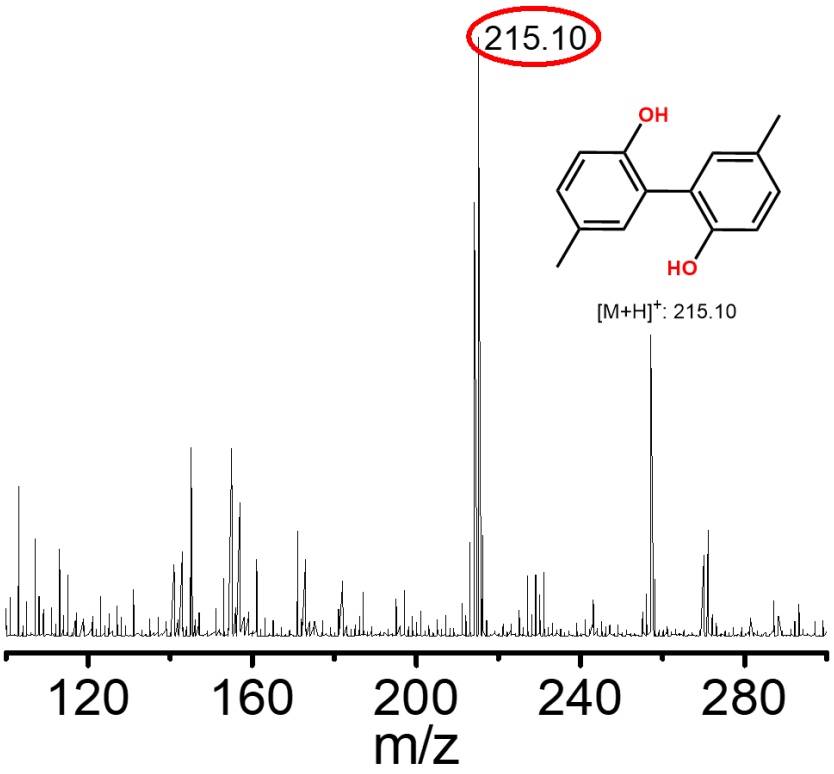

Fig. S39: Product analysis of the reaction of **5** with 50 eq. *p*-cresol by APCI-MS. *Conditions to generate **5**: 2.0 mM **4** in 3:1 $CH_3CN:H_2O$ + 20 eq. mCPBA and 140 eq. aqueous NaCl at room temperature.*

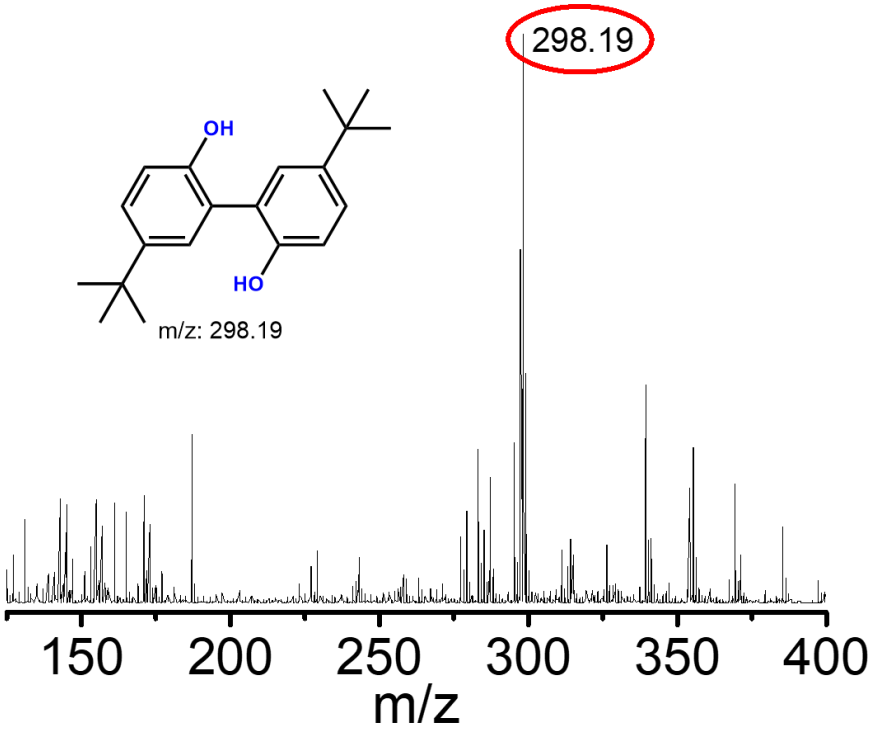

Fig. S40: Product analysis of the reaction of **5** with 50 eq. 4-(*tert*-butyl)phenol by APCI-MS. *Conditions to generate **5**: 2.0 mM **4** in 3:1 $CH_3CN:H_2O$ + 20 eq. mCPBA and 140 eq. aqueous NaCl at room temperature.*

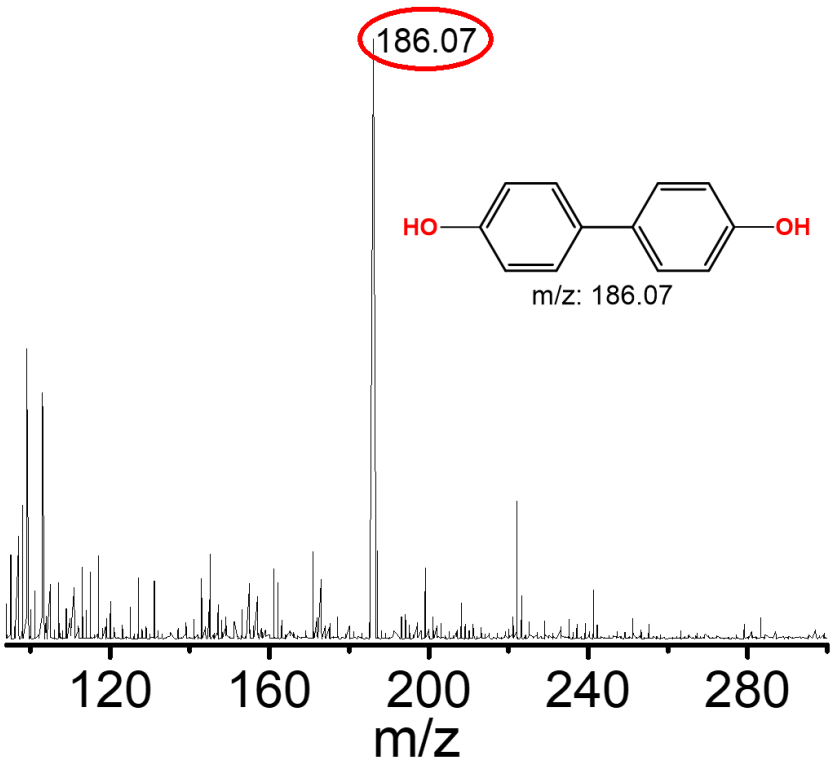

Fig. S41: Product analysis of the reaction of **5** with 50 eq. phenol by APCI-MS. *Conditions to generate **5**: 2.0 mM **4** in 3:1 CH_3CN:H_2O + 20 eq. mCPBA and 140 eq. aqueous NaCl at room temperature.*

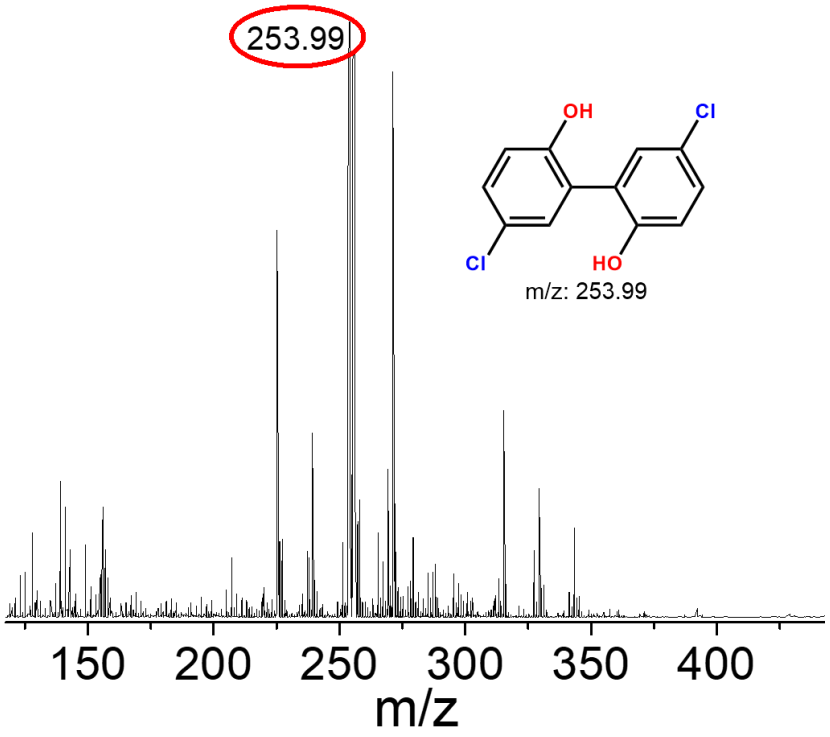

Fig. S42: Product analysis of the reaction of **5** with 10 eq. 4-chlorophenol by APCI-MS. *Conditions to generate **5**: 2.0 mM **4** in 3:1 CH_3CN:H_2O + 20 eq. mCPBA and 140 eq. aqueous NaCl at room temperature.*

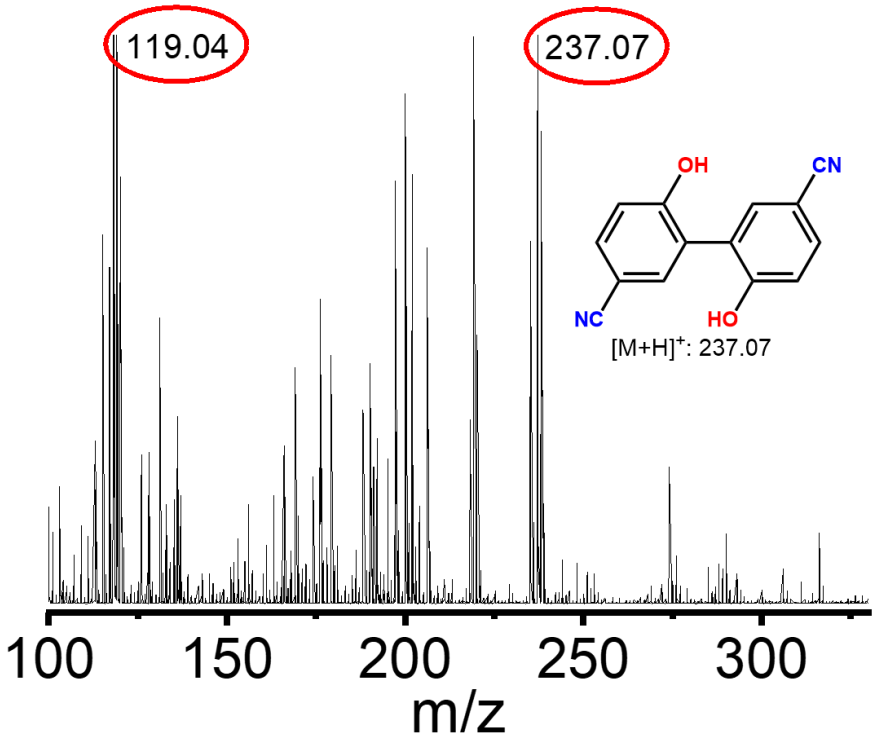

Fig S43: Product analysis of the reaction of **5** with 10 eq. 4-hydroxybenzonitrile by APCI-MS. *Conditions to generate **5**: 2.0 mM **4** in 3:1 $CH_3CN:H_2O$ + 20 eq. mCPBA and 140 eq. aqueous NaCl at room temperature.*

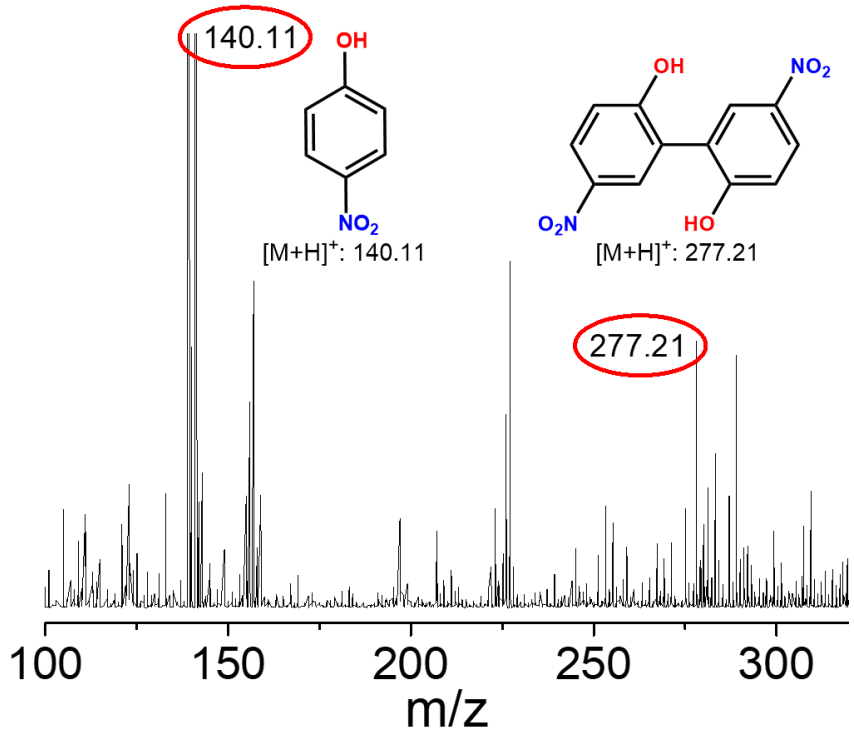

Fig. S44: Product analysis of the reaction of **5** with 10 eq. 4-nitrophenol by APCI-MS. *Conditions to generate **5**: 2.0 mM **4** in 3:1 $CH_3CN:H_2O$ + 20 eq. mCPBA and 140 eq. aqueous NaCl at room temperature.*

References:

1) R. Sharma, J. D. Knoll, P. D. Martin, I. Podgorski, C. Turro, J. J. Kodanko, *Inorg. Chem.,* 2014, **53**, 3272−3274.

2) S. Ohzu, T. Ishizuka, Y. Hirai, H. Jiang, M. Sakaguchi, T. Ogura, S. Fukuzumi, T. Kojima, *Chem. Sci.,* 2012, **3**, 3421-3431.